ISSN: 2754-4915

Journal of Material Sciences & Manufacturing Research

SCIENTIFIC Research and Community

Research Article

Open Access

Bead-Free PSF/PVP Blend Membrane as Potential Material for Water Desalination

William M Motswainyana[1*], Bakang F Modukanele[1] and Adewale O Adeloye[1,2]

[1]Botswana Institute for Technology Research and Innovation, Maranyane House, Plot 50654 Machel Drive, Gaborone, Botswana

[2]Department of Analytical, Colloid Chemistry and Technology of Rare Elements, al-Farabi Kazakh National University, Almaty, Republic of Kazakhstan

ABSTRACT

We herein report successful fabrication of bead-free PSF/PVP blend membrane using electrospinning technique. The membrane has been fully characterized by spectroscopic and microscopic techniques. Hydrophobicity of PSF was reduced by systematic addition of PVP to PSF, and confirmation of hydrophilicity of the PSF/PVP blend membrane was confirmed by contact angle and membrane water content measurements. Morphological images of the PSF/PVP fibers demonstrated that there is a critical, optimum PSF/PVP blending ratio, beyond which very large fibers start to form. Heat treatment of the membrane improved its mechanical strength and compactness. The membrane is a promising material for removing salt from saline water.

***Corresponding author**

William M Motswainyana, Botswana Institute for Technology Research and Innovation, Maranyane House, Plot 50654 Machel Drive, Gaborone, Botswana.

Received: September 03, 2024; **Accepted:** September 11, 2024; **Published:** October 30, 2024

Keywords: Electrospinning, Fabrication, Membrane, Hydrophilicity, Saline Water

Introduction

Desalination is a process of removing mineral components from water and often used to obtain potable water from seawater and brackish underground waters, which have mineral concentrations that reach up to 35,000 mg/L [1]. Membrane processes such as Microfiltration, Nanofiltration, Ultrafiltration and Reverse Osmosis are currently used for brackish water and seawater [1,2]. These filtration processes have been utilized in commercial water treatment systems for decades, with their global market reaching up to an estimated USD 26.3 billion in the year 2017 and an expected yearly growth of 8.5% [3]. The quality of filtration membrane has improved significantly with distinctive advantages such as low fouling properties, higher chemical resistance tolerance and good mechanical strength [1]. The membrane-based water filtration system also offers a more robust and consistent solid-liquid separation process to produce good quality potable water [1]. Separation of materials through the membrane depends on three basic principles: adsorption, sieving and electrostatic phenomenon [4,5]. The adsorption mechanism is based on hydrophobic interactions of the membrane and the analyte, and these interactions normally lead to more rejection because it causes a decrease in the pore size of the membrane [1,6]. The membrane system has its own inherent challenges. The system is susceptible to fouling and scaling [7,8]. Fouling is a result of concentration polarization that takes place when a rejected component increases at the boundary layer near the membrane surface [9]. The phenomenon can damage the membrane, thereby leading to a decrease in permeate flux and reduction in the life of a membrane [1,10]. On the other hand, membrane scaling occurs when dissolved substances precipitate from the solution and accumulate on the membrane surface or lodge in its pores [1]. This blockage eventually forms a cake layer when the membrane system is put into operation and decreases membrane performance [1,10].

Polyethesulfone (PES), Polysulfone (PSF), Polyvinyl difluoride (PVDF) and Polypropylene (PP) are some of the preferred membranes in water treatment due to their robust mechanical, structural and chemical stability [11-13]. However, these polymeric membranes are not suitable for harsh conditions. Their surfaces are susceptible to fouling due to their hydrophobic nature, which is viewed as a setback in their application as membrane materials [11]. Research effort has already been directed towards fabricating nanofibers from pure PSF for water treatment. For example, PSF nanofiber membranes were reportedly obtained from 20 wt% PSF, and subsequently applied as pre-filters for particulate removal [14]. However, fiber formation was overshadowed by occasional formation of beads. The resultant nanofiber membranes possessed high porosity, which together with their high surface area produced high flux pre-filters with high loading capacity [14]. There is on-going research which is seeking to increase hydrophilic properties of PSF membrane surface. The existing reports include blending PSF with hydrophilic inorganic nanoparticles or grafting with hydrophilic and functional polymers to increase the surface hydrophilic and antifouling properties [15,16]. Blending of graphene oxide (GO) or graphene oxide-titanium dioxide (GO-TiO_2) mixture into the polysulfone matrix had been carried out through phase inversion method to enhance the hydrophilic and antifouling properties, thereby making the blended membrane more hydrophilic with an increase in permeability, retention and antifouling capacity [11]. Hydrophilicity was also achieved by blending PSF with titanium dioxide (TiO_2) via phase inversion

or hydrothermal method [17,18]. The produced nanofibers were used to make polysulfone ultrafiltration membranes in the presence of polyethylene glycol as pore forming agent. The composite membranes demonstrated promising performance in both permeability and antifouling property [18].

Recently, PSF based membranes blended with PVP were prepared to treat batik industrial wastewater [19]. The PSF/PVP membranes were prepared using the phase inversion method and the study aimed to observe the effect of adding PVP on PSF membrane permeability and antifouling performance on a laboratory scale through the ultrafiltration (UF) process [19]. The study proved that the addition of a very low amount of PVP can still affect the increase in membrane flux and hydrophilicity values [19]. Generally, blending can generate hydrophilic membranes which possess excellent separation performance, good thermal and chemical resistance to survive the harsh wastewater environments [19-21].

In this work, we herein report successful fabrication of bead-free hydrophilic PSF/PVP blend membrane, with a view to demonstrating that hydrophobicity of PSF can be reduced by systematic addition of PVP to PSF. The membrane was fabricated by electrospinning and has been fully characterized by spectroscopic and microscopic techniques. Whereas phase inversion is a commonly used approach to blend polymers, electrospinning is a unique fabrication technique, and a straightforward nanofiber production technology that can produce nanofibrous nonwovens in the order of few nanometers with superior mechanical properties and ease of functionalization [22,23]. Electrospun materials offer a high surface area to volume ratio, high porosity and permeability and controllable fiber diameters [22]. The PSF/PVP membrane prepared in this work proved to be a promising material for removal of salinity, and to the best of our knowledge, this work represents the first investigation of electrospun PSF/PVP membrane in water desalination.

Experimental

Materials

The polymers polysulfone, PSF (Mw = 35 000) and polyvinylpyrrolidone, PVP (Mw = 360 000) and the solvent N, N-dimethylacetamide (DMAc, 99.9%), were purchased from Sigma-Aldrich and were used as received. Saline water was collected from a borehole in Kang village (Kgalagadi District), Botswana. A simple filtration set up was built in our laboratory.

Fabrication of PSF/PVP Membranes

Electrospinning experiments were carried out on a FLUIDNATEK LE-100 electrospinning unit. PSF/PVP spinning solution was prepared by dissolving PSF and PVP in 20 mL N, N-dimethylacetamide. A homogeneous solution was attained after 12 h of stirring at room temperature. Fiber formation was achieved by electrospinning the solutions under high voltage. The suitable voltage required to create a Taylor cone was within the range 25-30 kV, and the applied voltage transformed the polymer solution into a charged jet stream. The polymer jet streams were deposited on a rotating or stationery collector. Furthermore, the suitable feed was established to be in the range 1.0-2.8 mL/hr, while the sufficient flight distance for the polymer jet fell within the range 15-25 cm. The membranes were heat treated in an oven at 190 °C for 4 h.

Membrane Characterization

Studies of viscosity, surface tension, pore size, mechanical strength, hydrophilicity and thermal stability were performed by means of a Brookfield Viscometer, Force Tensiometer, Porolux 500 Porometer, MTS Criterion Tensile Tester, Optical Tensiometer, and Mettler Star System Differential Scanning Calorimetry respectively. Characterization and morphological analysis of the PSF/PVP fibers were performed using SHIMADZU IRTracer-100 Fourier Transform Infrared Spectrophotometer, SHIMADZU UV-2600 UV-VIS Spectrophotometer, Empyrean Pananalytical X-ray diffractometer and Gemini SEM 500 Scanning Electron Microscope.

Preliminary Desalination Experiments

Membrane water content measurements were performed by following the procedure described by Moradihamedani et al [24]. The membrane was pre-weighed, soaked in tap water for 24 h and weighed again.

The Water Content was Calculated using the Following Expression %Water content = $[W_w - W_d)/W_w]$ x 100; where: W_w and W_d are the weights of wet and dry membranes respectively [24].

The membrane permeability was studied using pure water flux measurements. The experiments were carried out under gravity. Fiber sheets were cut into disks of 7.5 cm diameter and the disks placed on a porous funnel, with a collector at the other end. In a typical permeability experiment, 350 mL of distilled water was added to the funnel, after which the permeate was collected after 4 min (Figure 1A).

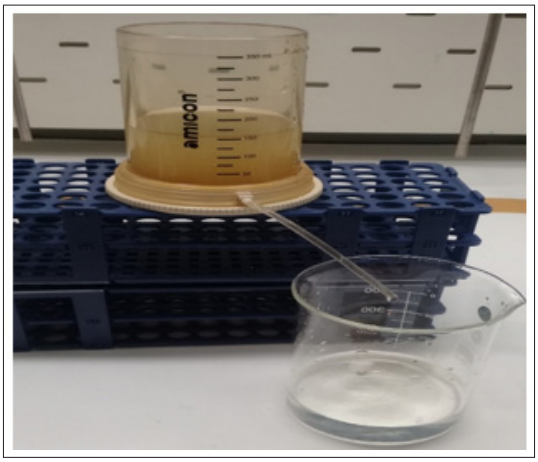

Figure 1A: Permeability and Separation Performance Set Up (Membrane Thickness = 0.252 mm, Diameter = 7.5 cm)

Permeability J was Calculated from the Expression

$J = Q/(A \times \Delta t)$; where: Q = quantity of permeate, A = surface area of membrane (m^2) and Δt is sampling time.

The performance of the membrane in the removal process was evaluated based on the flux measurement and the rejection percentage [24]. In a typical desalination experiment, 350 mL of borehole water was filtered in a porous funnel containing the PSF/PVP membrane and the filtrate collected on the other end. In another experiment, the pre-weighed membrane was simply soaked in borehole water for 24 h, dried at 70 °C for 48 h and weighed again to determine adsorption capability of the membrane. Salinity measurements were carried out using TDS measuring instrument.

Results and Discussion

Membrane Fabrication

An initial attempt was made to fabricate PSF fibers using 10, 18, 20, 22 and 25 wt% PSF polymer solutions. However, the fibers were marred by countless, spherical beads and poor fiber forming ability. Bead formation is the most common type of defect encountered in electrospun fibers, but effects of parameters such as polymer molecular weight, solvent, weight concentration and salt additives on the number and morphology of beads in the electrospinning process have not been studied quite substantially [25-28]. Qualitatively, beads may be expected at times during the electrospinning whenever the surface tension forces tend to overcome the forces that favor the elongation of the continuous jet [26]. Theoretical analysis of the mechanism of bead formation has been attempted and the analysis predicted two modes of instability that could develop in extending the jet: Rayleigh instability, which is mostly governed by the surface tension, and the conducting instability governed mainly by the electrical conductivity of the fluid [26]. Yuan et al and Khan & Kafiah suggested that lower viscosity and conductivity of the lower concentration PSF solutions could possibly be the causes of bead fiber morphology [29,30]. These beads disappeared as the solution concentration increased beyond 25%(wt/vol) [29,30]. In view of the electrospinning factors highlighted above, different PSF/PVP blend ratios: 20:0, 18:2, 16:4, 14:6, 12:8 and 10:10 wt% were investigated. The PSF/PVP blend in DMAc gave a clear solution, which culminated in a clean white membrane following electrospinning of the clear solution (Figure 1B).

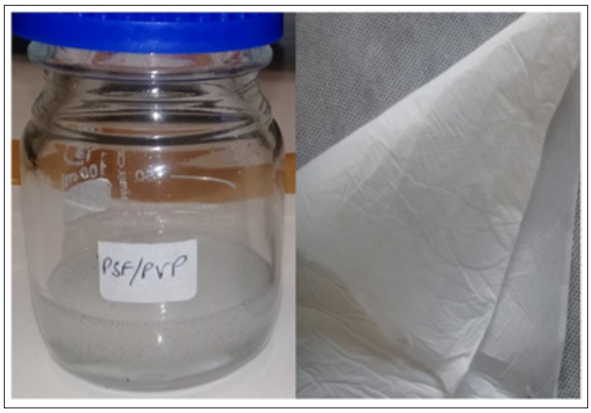

Figure 1B: Camera Images of PSF/PVP (16:4) Solution and PSF/PVP (16:4) Membrane

Remarkably, beads formation got suppressed when the PSF/PVP ratios 18:2, 16:4, 14:6, 12:8 wt% were applied. However, at 10:10 wt%, the fibers became very thick with occasional beads, suggesting that the ratio gave poor blending. Viscosity measurements showed that 20 wt% PSF had low viscosity, thereby making it susceptible to splitting and stretching during spinning, leading to beaded fibers. As PVP concentration increased from 2 to 8 wt%, the solution viscosity of PSF/PVP blend almost doubled. This general pattern suggested that the polymer jet would overcome splitting and stretching, thereby supporting the fabrication of bead-free and continuous fibers. Conversely, surface tension measurements returned a high surface tension value for 20 wt% PSF. However, these values increased as PVP concentration in the PSF/PVP blend increased from 2 to 8 wt%, thereby facilitating the production of bead-free fibers. Solution viscosity and surface tension measurements are provided in Table 1.

Table 1: Solution Viscosity and Surface Tension Measurements of PSF/PVP Blends

Blend ratio PSF/PVP	Viscosity (cP)	Surface Tension (mNm^{-1})
20:0	270	35.98
18:2	585	35.27
16:4	660	35.19
14:6	1398	34.65
12:8	2439	34.19
10:10	2670	33.49

Membrane Characterization

SEM Analysis of Membranes

Untreated Membranes

SEM images of PSF/PVP (18:2), PSF/PVP (16:4) and PSF/PVP (10:10) wt% fibers demonstrated continuous fibers of varying thickness, and the fiber thickness became extremely large as the PSF/PVP blend ratio approached 10:10 wt% (Figure 2).

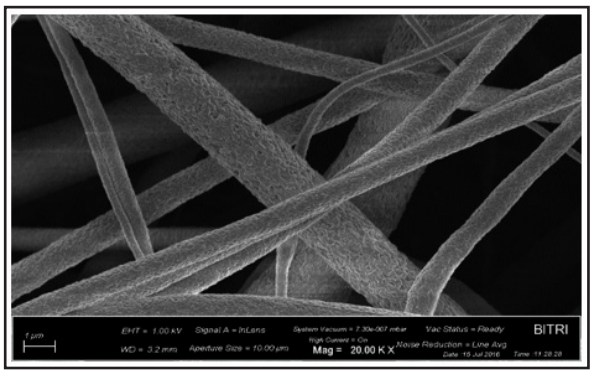

Figure 2A: SEM Image of PSF/PVP (18:2) Fibers

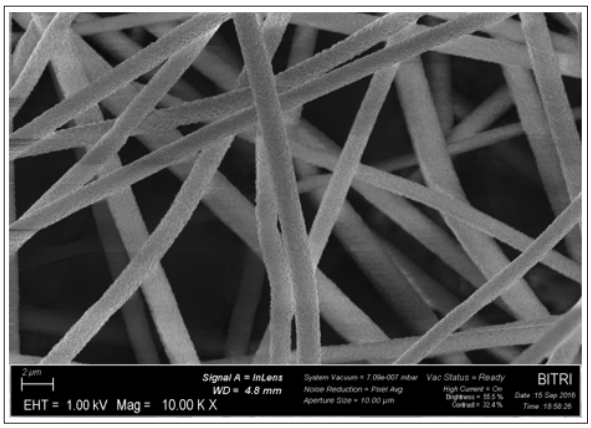

Figure 2B: SEM Image of PSF/PVP (16:4) Fibers

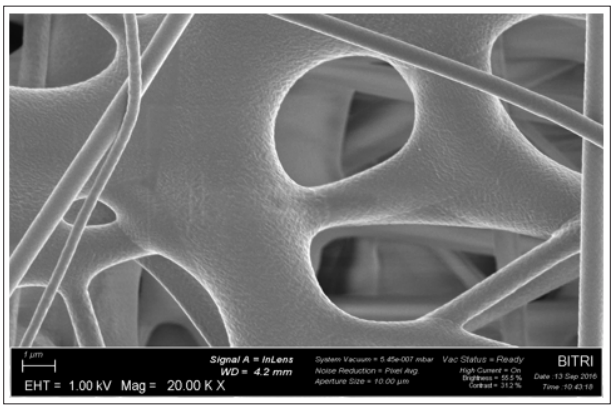

Figure 2C: SEM Image of PSF/PVP (10:10) Fibers

Heat Treated Membranes

PSF/PVP membranes were heat treated with a view to improve the mechanical strength and membrane compactness [31-33]. The membranes were heated in an oven at 190 °C for 4 h. The selected temperature is above glass transition temperatures of PSF (185 °C), PVP (188 °C) and boiling point of DMAc (165 °C). Generally, heating results in diffusion of the solvent to the surface of the nanofibers, thereby giving better contact between the membrane fibers. The morphology of the fibers changed completely and demonstrated better contact between the fibers after heat treatment (Figure 3). However, when the membranes were heated beyond 6 h, they disintegrated, forming grass-like flakes (Figure 3C), thereby suggesting that there is heating threshold beyond which heating affects membrane integrity.

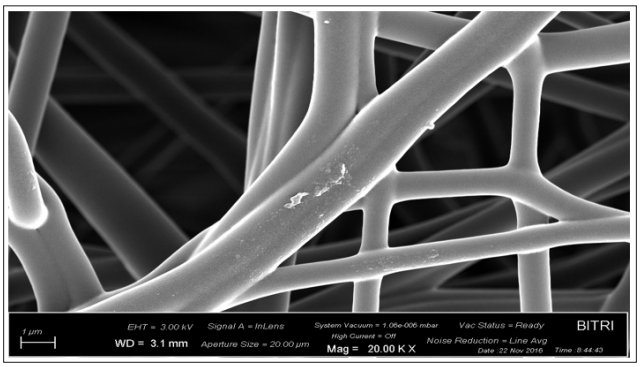

Figure 3A: SEM Image of PSF/PVP (18:2) Fibers after 4 h of Heat Treatment

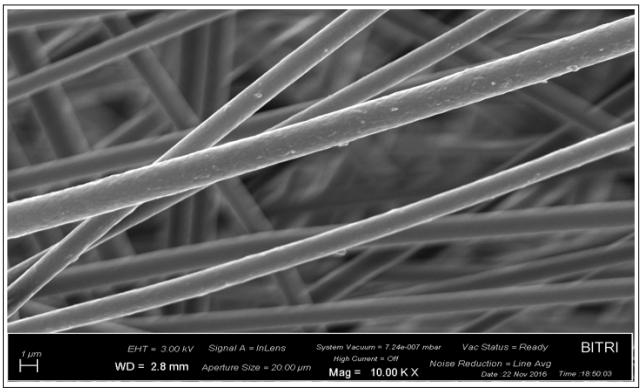

Figure 3B: SEM of PSF/PVP (16:4) Fibers after 4 h of Heat Treatment

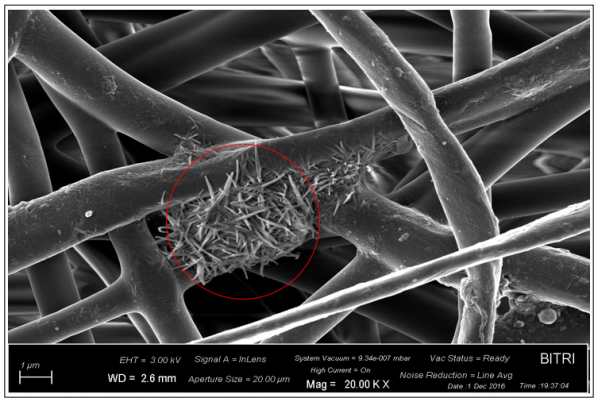

Figure 3C: SEM of PSF/PVP (16:4) Fibers after 6 h of Heat Treatment

Mechanical Strength, Porosity Measurements and Thermal Analysis

Mechanical properties of both non-heated and heated PSF/PVP blends were determined by applying a gradually increasing tensile force to the sample along its long axis until a deformation and rupture occurred. For non-heated membranes, the membranes exhibited high tensile stress and high elongation to break (Table 2A). Tensile stress decreased in the PSF/PVP blend membranes as PVP concentration increased. PSF/PVP (10:10) material remained the weakest with poor stretching ability, which could be attributed to its high porosity. However, there was a very significant increase in mechanical strength of the PSF/PVP membranes after heating, thereby suggesting that heat treatment improves membrane mechanical stability. The pore sizes of the membranes also got reduced during heat treatment (Table 2B), which could be attributed to the alignment of the molecules of the membranes in response to the heating effect [31]. It is therefore proffered that heat treatment adjusts membrane pore sizes and improves selectivity and mechanical strength [31,32].

Table 2A: Mechanical Strength Data for Non-Heated and Heat Treated PSF/PVP Membranes

Blend ratio PSF/PVP	Non-heated membrane		Heat treated membrane	
	Peak stress (MPa)	Strain at break (%)	Peak stress (MPa)	Strain at break (%)
20:0	15.3	65.59	-----	----
18:2	13.7	45.14	21.9	13.6
16:4	11.8	29.13	19.3	11.2
14:6	3.1	17.08	18.9	9.5
12:8	1.9	14.85	13.3	7.0
10:10	1.6	12.34	12.7	5.7

Table 2B: Porosity Determination of PSF/PVP Membranes before and after Heat Treatment

Blend ratio PSF/PVP	Non-heated membrane		Heat treated membrane	
	Smallest pore size (µm)	Bubble point size (µm)	Smallest pore size (µm)	Bubble point size (µm)
18:2	3.855	6.398	3.099	6.399
16:4	4.822	9.598	3.999	6.666
14:6	6.398	9.599	4.200	6.390
12:8	6.422	9.597	4.950	5.998
10:10	6.490	9.598	3.670	5.999

FTIR Analysis

Blending of PSF with PVP was justified by FTIR analysis of the membranes to identify the vibration frequency peaks of PSF and PVP before and after blending. FT-IR spectra of PSF, PVP and PSF/PVP (16:4) blend are presented in Figure 4. Absorption bands due to ring stretching vibrations in PSF were observed at 1586, 1490, 1318 and 1243 cm^{-1}, which was ascribed to the ν(C = C), ν(C – H), ν(CH_3), and ν(C – O) respectively [34]. The other observed bands at 1151 and 1013 cm^{-1} were attributed to ν(S = O) and ν(C – O) for the sulphone and ethereal groups in PSF. The IR spectrum of free PVP showed absorption bands at 1692, 1558, 1507, 1419 and 1287 cm^{-1}. These bands were assigned to the ν(C = O), ν(C = C), ν(C – N), ν(C – H), and ν(CH_2) vibrations respectively [35]. For the PSF/PVP polymer blend, three prominent features were observed in the spectrum: a shift to lower vibration frequency from 1692 to 1683 cm^{-1} in the C=O band, complete loss of vibration frequency peak at 1287 cm^{-1} (–CH_2–) in PVP, and associated decrease in intensity of these signals [34].

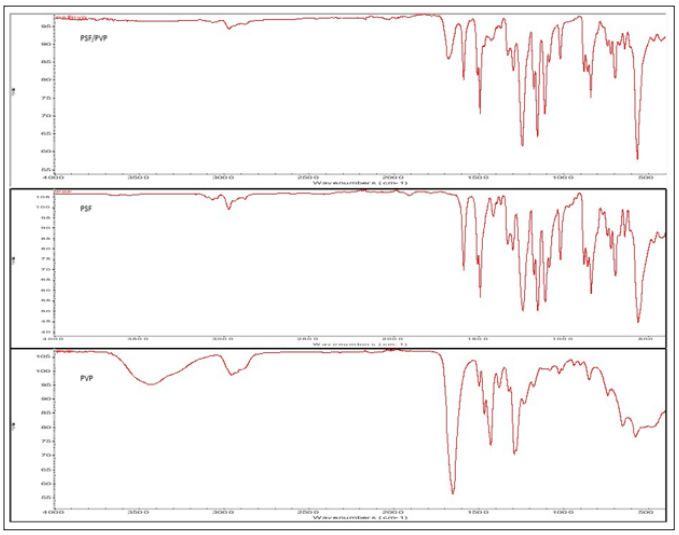

Figure 4: FTIR characterization of PSF, PVP and PSF/PVP blend

Surface Wetting Characteristics and Membrane Water Content

Surface wetting characteristics of neat PSF and PSF/PVP blend membranes were established to deduce the extent to which hydrophobicity of PSF was altered. This property generally quantifies wettability of a solid surface by a liquid via the Young's Equation, and its interpretation is such that low contact angle values indicate that the liquid spreads on the surface well while high contact angle values demonstrate poor spreading [35,36]. Neat PSF membrane (20 wt%) recorded a high contact angle of 89.90°, thereby justifying its hydrophobic nature. The contact angle for PSF/PVP 18:2 blend decreased to 87.02°, therefore suggesting that PSF/PVP 18:2 became slightly hydrophilic due to the incorporation of PVP. A more significant increase in hydrophilicity was observed in the PSF/PVP 16:4 (49.81°) blend as PVP concentration doubled. Furthermore, the PSF/PVP 10:10 membrane contact angle value of 17.64º represented an extremely hydrophilic polymer blend.

Membrane water content measurements were performed to confirm hydrophilicity of the membranes. All the membranes recorded % water content above 90%. The PSF/PVP 12:8 membrane exhibited the highest water content (99.0%) due to its high PVP concentration. The % water content increased as PVP concentration increased. However, the trend was somehow lost in PSF/PVP 10:10 membrane despite its high-water content (98.5%), which was not surprising because it was already established that a 10:10 ratio gave poor blending of PSF with PVP. Contact angle and membrane water content measurements are provided in Table 3.

Table 3: Hydrophilicity and Membrane Water Content Measurements of PSF/PVP Blends

Blend ratio PSF/PVP	Contact Angle (°)	% Water content
20:0	89.90	0.00
18:2	87.02	94.7
16:4	49.81	97.3
14:6	33.19	98.6
12:8	25.04	99.0
10:10	17.64	98.5

Removal of Salinity from Borehole Water

Kgalagadi, a desert region with lack of perennial water bodies relies solely on groundwater, but the water is saline in nature due to chemical accumulation, generally making the water unsuitable for human consumption. The salinity level of the borehole water in Kgalagadi is high (over 6 000 mg/L). Typically, natural water bodies contain different types of salts; NaCl, KCl, $MgSO_4$, $MgCl_2$, $CaCO_3$, and Na_2SO_4, which are the major targets for desalination processes [37].

Permeability tests on PSF/PVP membranes were carried out under gravity to demonstrate that the membranes are highly economical with low energy consumption. The quality of desalination membranes has in recent times improved significantly with distinctive advantages such as low fouling properties, higher chemical resistance tolerance and good mechanical strength, thereby offering a more robust and consistent solid-liquid separation process to produce good quality potable water [1]. The membranes exhibited good permeability, which was observed to increase with increasing PVP concentration in the blend. PSF/PVP (10:10) membrane recorded the highest flux, thereby verifying its high degree of wettability (Figure 5).

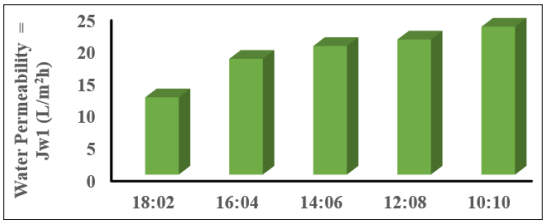

Figure 5: Water Permeability Test for PSF/PVP Membranes

The Results of Salinity Removal Experiments are Presented in Table 4, 5 and 6. Removal Efficiency was Calculated as Follows

$R (\%) = 1 – (C_f/C_i) \times 100\%$; where,
R = removal efficiency
C_i = initial concentration (feed)
C_f = final concentration (permeate)

Although the removal efficiency of the membrane was remarkably low (15%) when it was preliminarily subjected to salinity removal (Table 4), the PSF/PVP blend membrane demonstrated the potential to remove salt from borehole water. Conversely, PSF/PVP desalination membranes prepared by phase inversion have reportedly exhibited very high efficiencies of over 80% when the membranes were subjected to saline water or wastewater treatment [20,38]. However, our study has indeed confirmed the findings of Febriasari et al and others that, addition of PVP to PSF improves membrane flux and hydrophilicity values [20,37-39].

Considering that salinity removal was done via filtration of saline water under gravity, and that the pores size of the membranes is in the micrometer range, we propose adsorption as the possible mechanism through which the salt was removed from borehole water. Typically, size exclusion membranes should possess pore sizes of around 0.75 nm, which would be close to that of hydrated ions (Na^+, Mg^{2+}, Cl^-) for successful separation of salt and water [37]. When a PSF/PVP membrane was used repeatedly without refreshing, removal efficiency suffered greatly, reaching very low values of 5% (Table 5), thereby suggesting that the salt particles fouled the membrane and reduced the surface of interaction between membrane molecules and the salt [40].

Soaking the membrane in saline water was an attempt to demonstrate that the membrane could potentially act as an adsorbent for desalination which would require insignificant costs and energy [41]. The membrane returned a low removal efficiency of 10%. According to Dhumal & Sadgir, the process of adsorption in the earlier stages of the experiment is rapid since the accessibility of unoccupied regions on the surface of the adsorbent are providing ease of admission for ions [41]. However, as the available active sites become saturated with ions, it gradually reduces the removal rate of adsorption after achieving equilibrium [42]. It can thus be argued that the 10% removal efficiency was realized in the earlier stages of the experiment. Though its removal efficiency was quite low (around 15%) (Table 6), the membrane still demonstrated some capacity to remove salt from borehole water, thereby giving the researchers an interesting result to ponder on.

Table 4: Salinity Removal Experiments when a new Membrane was Used in Each Run

Run	Salinity before (mg/L)	Salinity after (mg/L)	% Salt removal
1	6 060	5 132	15.3
2	6 060	5 120	15.5
3	6 060	5 125	15.4
4	6 060	5 110	15.7

Table 5: Salinity Removal Experiment when the Membrane was not Changed

Run	Salinity before (mg/L)	Salinity after (mg/L)	% Salt removal
1	6 060	5 110	15.7
2	6 060	5 422	10.5
3	6 060	5 588	7.8
4	6 060	5 760	5.0

Table 6: Salinity Removal Experiment by Soaking Membrane in Saline Water

Run	Salinity before (mg/L)	Salinity after (mg/L)	% Salt removal
1	6 060	5 424	10.5
2	6 060	5 466	9.8
3	6 060	5 448	10.1
4	6 060	5 436	10.3

A PSF/PVP membrane that was used in salinity removal experiment was taken for SEM imaging to confirm interaction of the membrane with the salt. SEM image showed presence of white crystals within the fiber structures (Figure 6A), thereby suggesting that the membrane possesses capacity to remove salt from saline water through adsorption. Furthermore, EDX analysis of the same membrane showed presence of Na^+ and Cl^- in borehole water in an almost 1:1 ratio of the elemental concentrations (Figure 6B).

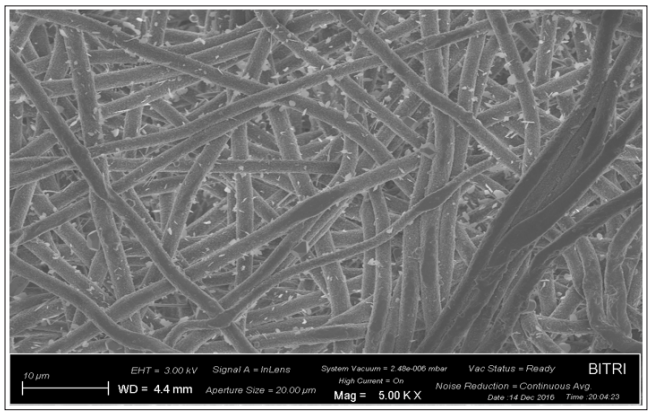

Figure 6A: SEM Image of PSF/PVP Membrane after Removing Salinity from Borehole Water

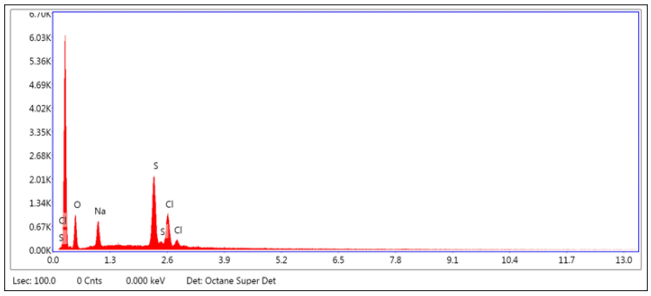

Figure 6B: EDX Analysis of PSF/PVP Membrane

Considering the Data and Observations Made above, we Herein Propose the Following Reaction Mechanism for the Interaction between PSF/PVP Membrane Surface and Sodium Chloride

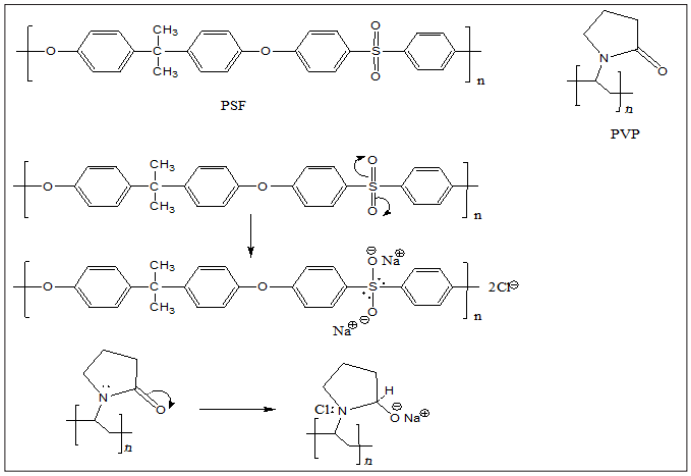

Scheme 1: Proposed reaction mechanism for PSF/PVP composite membrane with NaCl in saline water

According to our proposed mechanism (Scheme 1), the main adsorption takes place at the sulfone group, where sodium ions bind with the electron deficient oxygen atoms. The electron-rich sulphur atom containing two lone pairs of electrons shares these electrons with the incomplete orbital shell of chlorine atoms to form a Lewis structure (SCl_2) covalent bond. A similar adsorption mechanism occurred with the PVP polymer. Furthermore, the lone pair electrons on the nitrogen atom are shared with the incomplete orbital of the chlorine atom to form a covalent bond.

Conclusion

Bead-free PSF/PVP membrane has been successfully prepared by electrospinning. Contact angle measurements showed that there was significant increase in hydrophilicity when PSF/PVP blend ratio reached 10:10 wt%. Tensile stress was observed to decrease as PVP concentration in the PSF/PVP increased. Furthermore, the membranes exhibited good permeability, which was observed to increase with increasing PVP concentration in the blend. PSF/PVP (10:10) membrane recorded the highest flux, thereby verifying its high degree of wettability. The membrane was heat treated with a view to adjusting its pore sizes and improving its mechanical strength and compactness. However, heating the membrane beyond 6 h resulted in disintegration of the membrane, thereby suggesting that there is heating threshold beyond which heating affects membrane integrity. Though the removal efficiency was quite low, the PSF/PVP blend membrane demonstrated some potential to remove salt from borehole water. Against this background, the researchers propose adsorption as the possible interaction through which the salt was removed from borehole water. An improvement, such as reduction of the membranes pore sizes to nanometer range would increase separation efficiency of the membrane.

Acknowledgements

The authors gratefully acknowledge the financial support from Botswana Institute for Technology Research and Innovation.

Author Contribution Statement

Conceptualization, methodology, investigation, writing and review of the manuscript were done by WMM, BFM and AOA. Furthermore, all authors have read and consented to the publication of the manuscript.

References

1. Othman NH, Alias NH, Fuzil NS, Marpani F, Shahruddin MZ, et al. (2022) A Review of the Use of Membrane Technology Systems in Developing Countries. Membranes 12: 30.
2. Nqombolo A, Mpupa A, Moutloali RM, Nomngongo PN (2018) Wastewater Treatment Using Membrane Technology. Wastewater and Water Quality 29-40.
3. Ding H, Zhang J, He H, Zhu Y, Dionysiou DD, et al. (2021) Do membrane filtration systems in drinking water treatment plants release nano/microplastics? Science of Total Environment 755: 142658.
4. Padaki M, Murali RS, Abdullah MS, Misdan N, Moslehyani A, et al. (2015) Membrane technology enhancement in oil–water separation. A review. Desalination 357: 197-207.
5. Zhao D, Yu Y, Chen JP (2016) Treatment of lead contaminated water by a PVDF membrane that is modified by zirconium, phosphate and PVA. Water Research 101: 564-573.
6. Li K, Huang T, Qu F, Du X, Ding A, et al. (2016) Performance of adsorption pretreatment in mitigating humic acid fouling of ultrafiltration membrane under environmentally relevant ionic conditions. Desalination 377: 91-98.
7. Ahmed F, Lalia BS, Kochkodan V, Hilal N, Hashaikeh R (2016) Electrically conductive polymeric membranes for fouling prevention and detection: A review. Desalination 391: 1-15.
8. Zinadini S, Gholami F (2016) Preparation and characterization of high flux PES nanofiltration membrane using hydrophilic nanoparticles by phase inversion method for application in advanced wastewater treatment. Journal of Applied Research in Water and Wastewater 3: 232-235.
9. Koseoglu H, Guler E, Harman BI, Gonulsuz E (2018) Water flux and reverse salt flux. Membrane-Based Salinity Gradient Processes for Water Treatment and Power Generation 57-86.
10. Laohaprapanon S, Vanderlipe AD, Doma BT, You SJ (2017) Self-cleaning and antifouling properties of plasma-grafted poly (vinylidene luoride) membrane coated with ZnO for water treatment. Journal of the Taiwan Institute of Chemical Engineers 70: 15-22.
11. Nguyen HTV, Ngo THA, Do KD, Nguyen MN, Dang NTT, et al. (2019) Preparation and Characterization of a Hydrophilic Polysulfone Membrane Using Graphene Oxide. Journal of Chemistry 2019: 1-10.
12. Katheresan V, Kansedo J, Lau SY (2018) Efficiency of various recent wastewater dye removal methods: A review. Journal of Environmental Chemical Engineering 6: 4676-4697.
13. Salim N, Siddiqa A, Shahida S, Qaisar S (2019) PVDF based Nanocomposite Membranes: Application towards Wastewater Treatment. Madridge Journal of Nanotechnology and Nanoscience 4: 139-147.
14. Gopal R, Kaur S, Feng CY, Chan C, Ramakrishna S, et al. (2007) Electrospun nanofibrous polysulfone membranes as pre-filters: Particulate removal. Journal of Membrane Science 289: 210-219.
15. Prabhu KB, Saidutta MB, Isloor AM, Hebbar R (2017) Improvement in performance of polysulfone membranes through the incorporation of chitosan-(3-phenyl-1h-pyrazole-4 carbaldehyde). Codent Engineering 4: 1403005.
16. Ravishankar H, Christy J, Jegatheesan V (2018) Graphene oxide (GO)-Blended polysulfone (PSF) ultrafiltration membranes for lead ion rejection. Membranes 8: 77.
17. Guo W, Ngo HH, Li J (2012) A mini-review on membrane fouling. Bioresource Technology 122: 27-34.

18. Nair AK, Shalin PM, Jagadeesh Babu PE (2015) Performance enhancement of polysulfone ultrafiltration membrane using TiO2 nanofibers. Desalination and Water Treatment 57: 10506-10514.
19. Febriasari A, Huriya, Ananto AH, Suhartini M, Kartohardjono S (2021) Polysulfone-Polyvinyl Pyrrolidone Blend Polymer Composite Membranes for Batik Industrial Wastewater Treatment. Membranes 11: 66.
20. Urkiaga A, Iturbe D, Etxebarria J (2015) Effect of different additives on the fabrication of hydrophilic polysulfone ultrafiltration membranes. Desalination and Water Treatment 56: 3415-3426.
21. Aili D Kraglund, Tavacoli MR, Chatzichristodoulou JC, Jensen JO (2020) Polysulfone-polyvinylpyrrolidone blend membranes as electrolytes in alkaline water electrolysis. Journal of Membrane Science 598: 117674.
22. Mohammad MA, Shirazi SB, Fereshteh M (2020) Electrospun Nanofibrous Membranes for Water Treatment. Advances in Membrane Technologies 226.
23. Chen H, Huang M, Liu Y, Meng L, Ma M (2020) Functionalized electrospun nanofiber membranes for water treatment: A review. Science of The Total Environment 739: 139944.
24. Moradihamedani P, Kalantaric K, Abdullaha AH, Morad NA (2016) High efficient removal of lead (II) and nickel (II) from aqueous solution by novel polysulfone/Fe3O4–talc nanocomposite mixed matrix membrane. Desalination and Water Treatment 57: 28900-28909.
25. Liu Y, He JH, Yu JY, Zeng HM (2008) Controlling numbers and sizes of beads in electrospun nanofibers. Polymer International 57: 632-636.
26. Mazoochi T, Hamadanian M, Ahmadi M, Jabbari V (2012) Investigation on the morphological characteristics of nanofibrous membrane as electrospun in the different processing parameters. International Journal of Industrial Chemistry 3: 1-8.
27. Li Z, Wang C (2013) One-Dimensional nanostructures: Electrospinning Technique and Unique Nanofibers. Springer Berlin Heidelberg 15-28.
28. Subrahmanya TM, Bin Arshad A, Lin PT, Widakdo J, Makari HK, et al. (2021) A review of recent progress in polymeric electrospun nanofiber membranes in addressing safe water global issues. Royal Society of Chemistry Advances 11: 9638-9663.
29. Yuan X, Zhang Y, Dong C, Sheng J (2004) Morphology of ultrafine polysulfone fibers prepared by electrospinning. Polymer International 53: 1704-1710.
30. Khan Z, Kafiah FM (2013) Preparation of Polysulfone Electrospun Nanofibers: Effect of Electrospinning and Solution Parameters. Conference on Membranes Science and Technology https://www.researchgate.net/publication/273098355_Preparation_of_Polysulfone_Electrospun_Nanofibers_Effect_of_Electrospinnng_and_Solution_Parameters.
31. Ali SS, Abdallah H (2012) Development of PES/CA Blend RO Membrane for Water Desalination. International Review of Chemical Engineering 4: 316-323.
32. Feng S, Kondo S, Kikuchi T, Christiani L, Hwang B, et al. (2019) Development of a Heat-Treated Polymer-Polymer Type Charge-Transfer Blend Membrane for Application in Polymer Electrolyte Fuel Cells. ACS Applied Energy Materials 2: 8715-8723.
33. Pagno V, Modenesa AN, Dragunski DC, Fiorentin Ferrari LD, Caetano J, et al. (2020) Heat treatment of polymeric PBAT/PCL membranes containing activated carbon from Brazil nutshell biomass obtained by electrospinning and applied in drug removal. Journal of Environmental Chemical Engineering 8: 104159.
34. Aili D, Kraglund MR, Tavacoli J, Chatzichristodoulou C, Jensen JO (2020) Polysulfone polyvinylpyrrolidone blend membranes as electrolytes in alkaline water electrolysis. Journal of Membrane Science 598: 117674.
35. Polini A, Yang F (2017) Physicochemical characterization of nanofiber composites. Nanofiber Composites for Biomedical Applications 97-115.
36. Carrier O, Bonn D (2015) Contact Angles and the Surface Free Energy of Solids. Droplet Wetting and Evaporation 15-23.
37. Dutta S, de Luis RF, Goscianska J, Demessence A, Ettlinger R, et al. (2023) Metal-Organic Frameworks for Water Desalination. Advanced Functional Materials 2304790.
38. Ponnaiyan P, Nammalvar G (2020) Enhanced performance of PSF/PVP polymer membrane by silver incorporation. Polymer Bulletin 77: 197-212.
39. Xie P, de Lannoy CF, Ma J, Wang Z, Wang S, et al. (2016) Improved chlorine tolerance of a polyvinyl pyrrolidone-polysulfone membrane enabled by carboxylated carbon nanotubes. Water Research 104: 497-506.
40. Alaei Shahmirzadi MA, Hosseini SS, Luo J, Ortiz I (2018) Significance, evolution and recent advances in adsorption technology, materials and processes for desalination, water softening and salt removal. Journal of Environment Management 215: 324-344.
41. Dhumal R, Sadgir P (2023) Bioadsorbents for the removal of salt ions from saline water: a comprehensive review. Journal of Engineering and Applied Science 70: 1-21.
42. Shahawy A, Ahmed IA, Wagdy R, Ragab AH, Shalaby NH (2021) Phragmites australis (Reed) as an efficient, ecofriendly adsorbent for brackish water pre-treatment in reverse osmosis: A kinetic study. Molecules 26: 6061.